Synchronization and extinction in cyclic games with mixed strategies

Ben Intoy and Michel Pleimling
Department of Physics, Virginia Tech, Blacksburg, Virginia 24061-0435, USA
(Received 22 February 2015; published 22 May 2015)

We consider cyclic Lotka-Volterra models with three and four strategies where at every interaction agents play a strategy using a time-dependent probability distribution. Agents learn from a loss by reducing the probability to play a losing strategy at the next interaction. For that, an agent is described as an urn containing β balls of three and four types, respectively, where after a loss one of the balls corresponding to the losing strategy is replaced by a ball representing the winning strategy. Using both mean-field rate equations and numerical simulations, we investigate a range of quantities that allows us to characterize the properties of these cyclic models with time-dependent probability distributions. For the three-strategy case in a spatial setting we observe a transition from neutrally stable to stable when changing the level of discretization of the probability distribution. For large values of β, yielding a good approximation to a continuous distribution, spatially synchronized temporal oscillations dominate the system. For the four-strategy game the system is always neutrally stable, but different regimes emerge, depending on the size of the system and the level of discretization.

DOI: 10.1103/PhysRevE.91.052135 PACS number(s): 05.70.Ln, 05.50.+q, 64.60.De, 89.75.Kd

I. INTRODUCTION

Evolutionary game theory is nowadays a well-established approach to model and study complex biological and ecological systems [1–4]. Of special importance are thereby spatial systems, as they give rise to novel and rich phenomena, ranging from the formation of complicated space-time patterns, in the form of spirals or cluster coarsening, to the emergence of nested ecological niches [5–8]. Most studies published in this context focused on spatial cyclic games with three [9–32] or four species [33–38], but there have also been some attempts to generalize this to more complex networks with a larger number of species [7,35,39–57]. In general, these competition models assume that an agent will play a single strategy when confronted by another agent. The act of playing a single strategy is known in classical game theory as a pure strategy [58]. In the literature on population and evolutionary dynamics a strategy is associated with a single species and/or genotype. Depending upon the model dynamics, a losing agent will either be removed completely or will replace the losing strategy with the winning pure strategy.

In game theory, other than pure strategies, there is also the notion of mixed strategies [58]. A mixed strategy is when at every interaction an agent picks and plays one of the possible pure strategies using a probability distribution. Mixed strategies are sometimes encountered in nature [59,60], but can be seen most readily in social systems where decision making is important [61,62]. Economics is another area where game theory with either pure or mixed strategies has been studied. A series of economics papers focus on modifications of the three-species rock-paper-scissors model (see, for example, [63–67]), whereas others tie three-strategy cyclic domination to the public goods game [68–73]. Some papers discuss spatial games in an economics setting, but usually only games with two pure strategies (prisoner's dilemma, snowdrift, and hawk and dove) are considered [74–77].

In this paper we study versions of the cyclic three- and four-strategy games where agents are selecting a strategy from a time-dependent probability distribution. Learning from a recent loss, an agent changes their probability distribution in such a way that it becomes less likely to play the losing strategy at the next interaction. As the emerging space-time properties in a spatial setting are of special interest, we focus in this work on agents that exist on a one-dimensional lattice and only interact with their two nearest neighbors. Some results are also presented for the well-mixed situation without an underlying spatial system.

In our implementation we describe every agent as an urn that contains β balls of three and four different types, respectively, corresponding to the different pure strategies. At every interaction one of these β balls is chosen randomly and the related strategy is played. If that strategy loses, the ball is replaced by a different ball representing the winning strategy. In that way the losing agent is less likely to play at the next interaction the losing strategy again. It should be noted that the value of β is a measure of discretization of the probability distribution, with the limit $\beta \to \infty$ yielding a continuous distribution. As we discuss in the following, changing the value of β has a strong impact on the properties of systems with cyclic domination. For example, for the three-species strategies we observe a transition from a neutrally stable system to a stable system when increasing β. In addition, in the limit of $\beta \gg 1$ the system synchronizes, yielding spatially extended coherent temporal waves. When considering four strategies, one always has a neutrally stable system, but the average time for strategy extinction displays different regimes, depending on the value of β and on the system size.

Our paper is organized in the following way. In the next section we present our models in more detail. Sections III and IV are devoted to our results, first for the three-strategy case and then for the four-strategy model. In order to elucidate the properties of our mixed-strategy spatial systems with cyclic domination and a time-dependent probability distribution we study a range of quantities: time-dependent densities, space-time covariances and related length scales, and average times for strategy extinction. We summarize and conclude in Sec. V.

II. MODELS

In the symmetric Lotka-Volterra model reactions are taking place with rate λ in a cyclic way between M different

species [78,79]:

$$X_i + X_{i+1} \xrightarrow{\lambda} X_i + X_i, \tag{1}$$

where X_i is an agent of species i, with $i = 1,\ldots,M$ and the cyclic identification $M+1 \equiv 1$. In the language of population dynamics, every species has one prey and is the prey of a single other species. The three-species case is special, as a reaction takes place whenever two agents of different types are selected. For cases with more than three species one has mutually neutral species that do not interact [79,80]. Cyclic Lotka-Volterra games can be played in the well-mixed case as well as on lattices where a variety of situations has been considered. For example, one can impose a strict site restriction with exactly one agent occupying each lattice site and reactions taking place between neighboring sites [78,79]. This can be coupled with exchanges of agents sitting on nearest-neighbor sites, in order to provide a mechanism for mobility [9,12]. Sometimes the site restriction is dropped so that every site can hold a variable number of agents that can diffuse and interact with agents on neighboring sites [16]. In the related systems with May-Leonard dynamics, the reaction (1) is replaced by two separate reactions [9,81] (usually with different rates)

$$\begin{aligned} X_i + X_{i+1} &\to X_i + 0, \\ X_i + 0 &\to X_i + X_i, \end{aligned} \tag{2}$$

where 0 indicates an empty site. In this scheme the number of agents in the system is a stochastic quantity that is only conserved on average.

We consider in the following versions of the three- and four-strategy cyclic Lotka-Volterra game with mixed strategies where at every interaction agents play one of the possible strategies using a time-dependent probability distribution. Imagine an agent as an urn that contains β balls of three (for the three-strategy version) or four (for the four-strategy case) different types. For a well-mixed system without a lattice structure we first choose two agents (urns) at random out of a total of N agents (urns) before choosing randomly a ball out of each selected urn. Depending on the types of balls selected, a reaction may take place with rate $\lambda = 1$ following the scheme (1). If the strategy played by one of the agents is beaten, then the losing ball is replaced by a ball of the winning type before the balls are put back into the urns. The losing agent therefore changes the probability distribution as a result of the loss by increasing (decreasing) the probability to play the winning (losing) strategy at the next interaction. For a spatial game we only consider the case with exactly one agent at every lattice site. In order to start an interaction we select an agent and one of their neighbors at random and then proceed as for the well-mixed case. In our simulations we define one time step to be $N\beta$ proposed updates.

One can view this scheme in a spatial setting as a version of the spatial cyclic Lotka-Volterra model with multiple occupancy of each site, but there are important differences. In the model discussed in [16] in the context of population dynamics, not only do individuals interact with agents on other lattice sites, but they also diffuse by jumping with a given probability to one of the neighboring sites. As a result, the number of individuals at each site fluctuates and only the average spatial density is constant. In our case, only interactions take place, so the number of balls at each site (which corresponds to the number of individuals at a given site in the model of [16]) is strictly conserved. As we will see in the following, this additional conservation law has a huge impact on the properties of our system.

III. MIXING OF THREE STRATEGIES

As already mentioned, the situation with three strategies is rather special, as every time two different strategies are played, there will be a losing and a winning strategy. In the following we show, both in the well-mixed case and on the ring, that for continuous probability distributions a synchronization of the strategies played by the different agents takes place. For a small number of balls per agent a transition in the stability properties of the lattice system is observed.

A. Mean-field equations for the well-mixed case

We first consider the mixed three-strategy game in a well-mixed system without spatial structure. Agent j is characterized by the number of balls of each type at their possession: (a_j,b_j,c_j), with $a_j + b_j + c_j = \beta$, where a_j is the number of balls of type A. The state of the system of N agents is then given by the number of balls of each type in possession of each agent, i.e., by the configuration

$$\{(a_n,b_n,c_n)\} = \{(a_1,b_1,c_1),\ldots,(a_j,b_j,c_j),\ldots,(a_N,b_N,c_N)\}. \tag{3}$$

The interaction scheme (1) with rates $\lambda = 1$ directly translates into the following master equation for the probability that the system is in state $\{(a_n,b_n,c_n)\}$ at time $\tau + 1$:

$$\begin{aligned} P(\{(a_n,b_n,c_n)\};\tau+1) = {} & \frac{1}{\beta^2}\frac{2}{N(N-1)} + \Bigg[\sum_j \sum_{i\neq j} a_i(b_j+1)P(\ldots,(a_i,b_i,c_i),\ldots,(a_j-1,b_j+1,c_j),\ldots;\tau) \\ & + \sum_j \sum_{i\neq j} b_i(c_j+1)P(\ldots,(a_i,b_i,c_i),\ldots,(a_j,b_j-1,c_j+1),\ldots;\tau) \\ & + \sum_j \sum_{i\neq j} c_i(a_j+1)P(\ldots,(a_i,b_i,c_i),\ldots,(a_j+1,b_j,c_j-1),\ldots;\tau) \Bigg] \\ & + \left(1 - \frac{1}{\beta^2}\frac{2}{N(N-1)} \sum_j \sum_{i\neq j} (a_i b_j + b_i c_j + c_i a_j)\right) P(\{(a_n,b_n,c_n)\};\tau), \end{aligned} \tag{4}$$

where the factor $\frac{2}{N(N-1)}$ takes into account the number of combined choices of the two agents i and j. The first three sums represent the reactions (1) through which the system enters the state $\{(a_n,b_n,c_n)\}$, while the last term represents the case where no reaction happens (when balls of the same type are pulled out for both agents) and the system stays in the same state.

We define the density of ball type A for agent j at time τ to be

$$A_j(\tau) = \sum_{\{(a_n,b_n,c_n)\}} \frac{a_j}{\beta} P(\{(a_n,b_n,c_n)\};\tau) \tag{5}$$

with similar equations for ball types B and C. Neglecting correlations, Eqs. (4) and (5) yield the equation (with similar equations found for the other ball types through symmetry)

$$\begin{aligned} A_k(\tau+1) - A_k(\tau) &= \sum_{\{(a_n,b_n,c_n)\}} \frac{a_k}{\beta}[P(\{(a_n,b_n,c_n)\};\tau+1) - P(\{(a_n,b_n,c_n)\};\tau)] \\ &= \sum_{\{(a_n,b_n,c_n)\}} \frac{1}{\beta^3}\frac{2}{N(N-1)}\sum_{i\neq k}(a_i b_k - c_i a_k)P(\{(a_n,b_n,c_n)\};\tau) \\ &= \frac{1}{N\beta}\left[2\left(\frac{1}{N-1}\sum_{i\neq k}A_i(\tau)\right)B_k(\tau) - 2\left(\frac{1}{N-1}\sum_{i\neq k}C_i(\tau)\right)A_k(\tau)\right]. \end{aligned} \tag{6}$$

Letting $t = \frac{\tau}{N\beta}$ and taking the continuum limit $\beta \to \infty$ so that $A_k(\tau+1) - A_k(\tau) \to \frac{1}{N\beta}\partial_t A_k(t)$ finally leads to the mean-field equations

$$\begin{aligned} \partial_t A_k(t) &= 2\left(\frac{1}{N-1}\sum_{i\neq k}A_i(t)\right)B_k(t) - 2\left(\frac{1}{N-1}\sum_{i\neq k}C_i(t)\right)A_k(t), \\ \partial_t B_k(t) &= 2\left(\frac{1}{N-1}\sum_{i\neq k}B_i(t)\right)C_k(t) - 2\left(\frac{1}{N-1}\sum_{i\neq k}A_i(t)\right)B_k(t), \\ \partial_t C_k(t) &= 2\left(\frac{1}{N-1}\sum_{i\neq k}C_i(t)\right)A_k(t) - 2\left(\frac{1}{N-1}\sum_{i\neq k}B_i(t)\right)C_k(t). \end{aligned} \tag{7}$$

As we show in the Appendix, the usual mean-field rate equations for the well-mixed rock-paper-scissors model are recovered if one takes in addition the limit of infinitely many agents $N \to \infty$.

Let us have a closer look at the simple case of two agents $N = 2$. Equations (7) can be easily written as

$$\begin{aligned} &\partial_t A_1 = 2(A_2B_1 - C_2A_1), \quad \partial_t A_2 = 2(A_1B_2 - C_1A_2), \\ &\partial_t B_1 = 2(B_2C_1 - A_2B_1), \quad \partial_t B_2 = 2(B_1C_2 - A_1B_2), \\ &\partial_t C_1 = 2(C_2A_1 - B_2C_1), \quad \partial_t C_2 = 2(C_1A_2 - B_1C_2). \end{aligned} \tag{8}$$

From $\partial_t(A_1 - A_2)$ we find

$$\begin{aligned} \partial_t(A_1 - A_2) &= 2[(A_2B_1 - C_2A_1) - (A_1B_2 - C_1A_2)] \\ &= -2(A_1 - A_2) \end{aligned} \tag{9}$$

as $A_i + B_i + C_i = 1$. Solving this differential equation yields

$$A_1(t) - A_2(t) = (a_1 - a_2)e^{-2t}, \tag{10}$$

where $a_1 = A_1(0)$ and $a_2 = A_2(0)$ are initial conditions. Similar equations are obtained for ball types B and C. It follows that whatever the initial conditions the difference in ball densities of the two agents vanishes exponentially fast, yielding a synchronization of the two agents. Although not presented here, the synchronization of more than two agents has also been studied in some detail (see [82]).

We can use the previous results to eliminate the densities of agent 2 and end up with the following three coupled nonautonomous differential equations for the ball densities of agent 1:

$$\begin{aligned} \partial_t A_1 &= 2(A_1B_1 - C_1A_1) + 2[(a_2 - a_1)B_1 - (c_2 - c_1)A_1]e^{-2t}, \\ \partial_t B_1 &= 2(B_1C_1 - A_1B_1) + 2[(b_2 - b_1)C_1 - (a_2 - a_1)B_1]e^{-2t}, \\ \partial_t C_1 &= 2(C_1A_1 - B_1C_1) + 2[(c_2 - c_1)A_1 - (b_2 - b_1)C_1]e^{-2t}. \end{aligned} \tag{11}$$

We note that in the long-time limit $t \to \infty$ we recover the mean-field rate equations for the well-mixed rock-paper-scissors game.

In Fig. 1 we compare these theoretical results (lines in the figure), obtained through numerical integration of the Eqs. (11), with results from stochastic simulations (symbols in the figure) for initial conditions $A_1(0) = 0.8$, $B_1(0) = 0.1$, $A_2(0) = 0.1$, and $B_2(0) = 0.8$. We find that the numerical integration results agree with the stochastic simulation very well; in analogy with the three-species well-mixed model [83], we expect the fluctuations for an individual agent to be proportional to $\beta^{-1/2}$. Even though the initial conditions are very different, the synchronization between the two agents

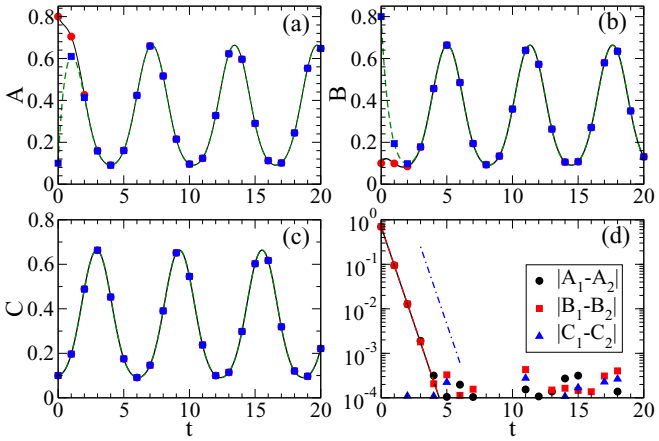

FIG. 1. (Color online) Time-dependent densities for a system of two agents obtained through numerical integration of Eqs. (11) (solid black line, agent 1; green dashed line, agent 2) and compared with results from stochastic simulations with $\beta = 10^7$ (red circles, agent 1; blue squares, agent 2). The same initial conditions $A_1(0) = 0.8$, $B_1(0) = 0.1$, $A_2(0) = 0.1$, and $B_2(0) = 0.8$ are used for both methods. In (d) the symbols represent the absolute values of the difference between strategy densities in the simulation data, while the lines are obtained from Eqs. (11). An exponentially fast synchronization is observed. The dot-dashed blue line indicates an exponential of slope -2.

is very rapid and the differences between the corresponding densities vanish exponentially [see Fig. 1(d)].

B. Numerical simulations on the ring

The simplest spatial system is the one-dimensional lattice with periodic boundary conditions. As discussed previously, every site of the ring is occupied by one agent who has at their disposal β balls. In the initial state every ball is assigned with the same probability one of three possible types corresponding to the three strategies A, B, and C. Once the system has been prepared in that way, pairs of neighboring sites are randomly selected and interactions take place following the scheme described above.

The dynamics can be readily visualized through space-time plots such as those shown in Fig. 2. Inspection of these plots for various numbers of balls β reveals an interesting transition in the shape of the space-time patterns. Whereas for three balls or fewer the system behaves like the standard Lotka-Volterra rock-paper-scissors game on the ring with immobile agents (which corresponds to $\beta = 1$) and exhibits coarsening processes that end when only one strategy fills the complete lattice [see Fig. 2(a)], for $\beta \geqslant 4$ a tiling structure appears where a tile indicates that a part of the system is dominated by one of the three strategies for a finite amount of time [see Fig. 2(b)]. It follows that every agent changes the most likely strategy after some time and that it becomes difficult for one strategy to dominate the system. This tiling structure is reminiscent of very similar patterns that are encountered when allowing in the one-dimensional rock-paper-scissors model for swapping of particles as an efficient mechanism for mobility [13]. As discussed further below (see Fig. 3), the tiling structure promotes coexistence and stabilizes the system, with only rare large stochastic fluctuations causing the finite system to go to an absorbing fixed point. When we further increase β, the tiles, corresponding to regions where one strategy dominates locally, decrease in size [see Fig. 2(c) for the case with $\beta = 6$]. This is accompanied by the emergence of grayish patches that indicate spatial regions where in the probability distribution the three strategies have similar weights. Finally, for large values of β, corresponding to a probability distribution that approximates a continuous distribution, the system rapidly synchronizes and spatial extended coherent temporal waves are formed, as shown in Fig. 2(d) for the example of $\beta = 100$ balls.

In order to relate the coarsening and tiling space-time patterns to different extinction regimes, we measure the average lattice domination time T, i.e., the average time at which only one of the strategies remains in the system. Figure 3 reveals that the average lattice domination time changes its dependence on the system size at the transition gleaned from the space-time plots. For $\beta \leqslant 3$ the average lattice domination time increases algebraically with the total number of balls $T \sim (N\beta)^b$, as shown by the straight lines in the log-log plot in Fig. 3(a), with the exponent $b = 1.93(2)$, $1.90(2)$, and $1.77(2)$ for $\beta = 1$, 2, and 3, respectively. As shown in Refs. [9,84,85], there is a direct correspondence between the system size dependence (exponential, algebraic, or logarithmic) of the lattice domination time of a system and its stability properties (stable coexistence, neutrally stable coexistence, or unstable coexistence). The observed algebraic dependence therefore indicates that the system is neutrally stable. We also note that the lattice domination time for a fixed value of $N\beta$ decreases for increasing β, indicating that the system becomes less stable. This trend is reversed when we enter the tiling regime [see Fig. 3(b)] as now for fixed $N\beta$ the lattice domination time strongly increases with β. In fact, the dependence of T on $N\beta$ changes to an exponential dependence for $\beta \geqslant 4$, as the system becomes a stable system [83].

Another quantity that allows us to gain insights into this transition is the total space-time covariance

$$C_0(x,t) = \frac{C_{AA}(x,t) + C_{BB}(x,t) + C_{CC}(x,t)}{3} \tag{12}$$

with

$$C_{AA}(x,t) = \frac{1}{N}\sum_i A_i(t)A_{i+x}(t) - \mu_A(t)\mu_A(t) \tag{13}$$

and similar expressions for $C_{BB}(x,t)$ and $C_{CC}(x,t)$. Here $\mu_A(t) = \frac{1}{N}\sum_i A_i(t)$ and similarly for μ_B and μ_C. Figure 4 shows this quantity after 1000 time steps since the preparation of the system for β ranging from 1 to 6 and system sizes between $N = 500$ and 10 000. For $\beta \leqslant 3$ the covariance displays the expected behavior for systems with domain ordering, with strong finite-size effects for small systems, as in many instances runs have already reached their final state (with one strategy filling the whole system) at $t = 1000$, and an exponential decay with the distance x for larger sizes when the coarsening system is still far from its final state. After the transition to the tiling regime [see Figs. 4(d)–4(f)] the initial decay becomes system size independent and is followed by a shoulder [see the data for $\beta = 6$ in Fig. 4(f)]. We relate this behavior to the typical sizes of the tiles whose spatial extensions are rather small and decrease with an increase of β.

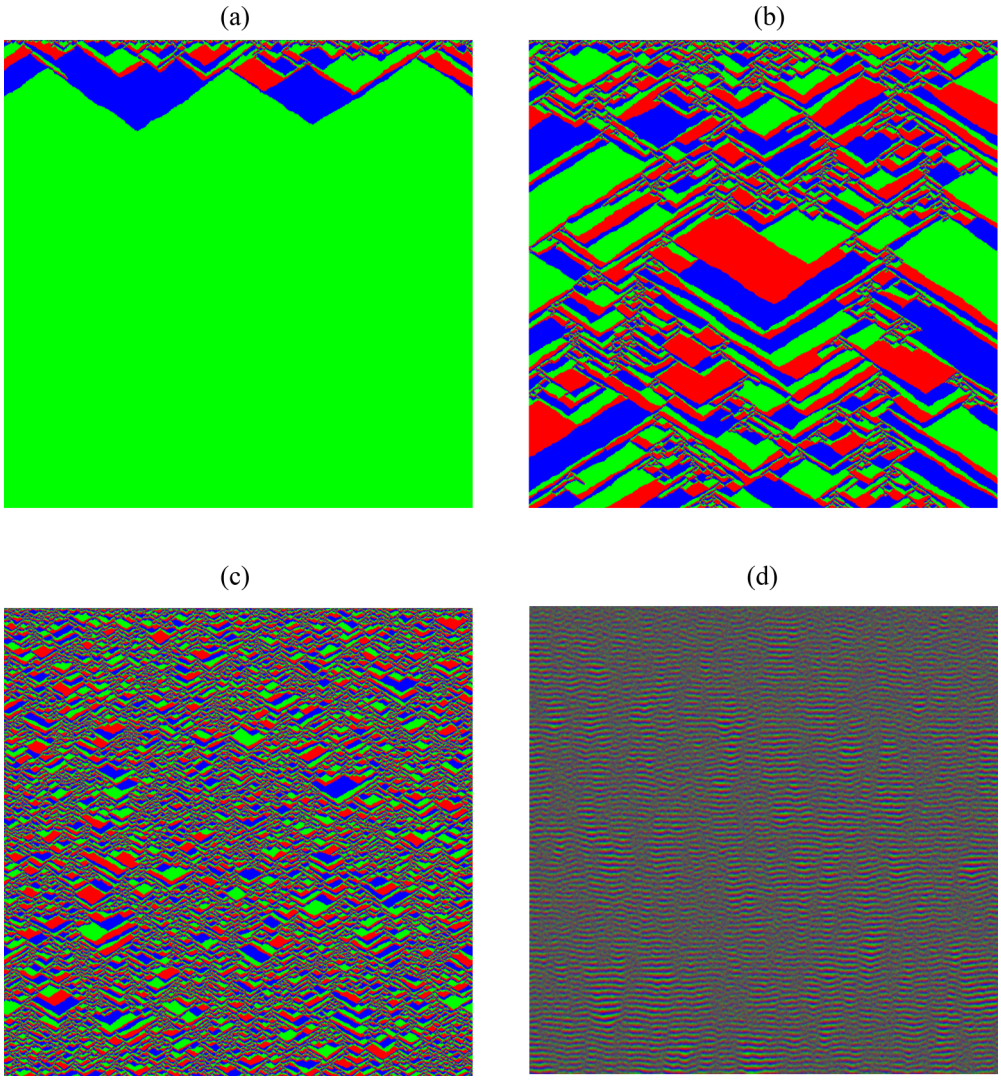

FIG. 2. (Color online) Space-time plots for three-strategy games on a ring with different numbers of balls β on each site: (a) $\beta = 3$, (b) $\beta = 4$, (c) $\beta = 6$, and (d) $\beta = 100$. Time progresses from top to bottom. For (a)–(c) 1000 time steps are shown for a system composed of 1000 sites, whereas for (d) we show 500 time steps for a system with 500 lattice points. To determine the color of a lattice site we use the RGB color model and map the percentage of A, B, and C to the percentage of the colors red, green, and blue, respectively. In this scheme a site that contains the same number of balls for all three species is assigned a grayish color.

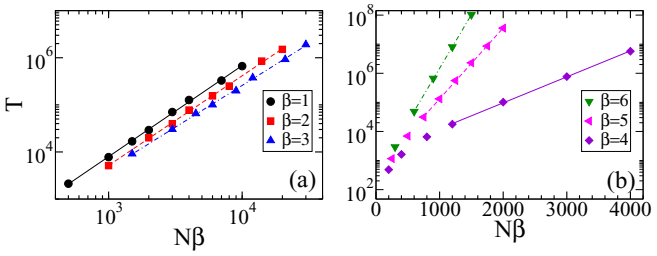

FIG. 3. (Color online) Average lattice domination time T as a function of the total number of balls $N\beta$ in the system. When changing the number of balls β per agent, a transition takes place between (a) an algebraic dependence on the total number of balls in the system for $\beta \leqslant 3$, indicating a neutrally stable system, and (b) an exponential dependence for $\beta \geqslant 4$, characterizing a stable system. Each data point results from an average over 2000 runs with different realizations of the noise. Error bars are smaller than the symbol sizes.

C. Spatial mean-field equations and synchronization

As we saw in Fig. 2(d) synchronization in space coupled with temporal oscillations sets in for a large number of balls β. As in the limit $\beta \to \infty$ the probability distribution becomes continuous, we can capture this effect through spatial mean-field equations.

Our starting point is the mean-field equations (7) for N agents in the well-mixed case with $\beta \to \infty$ that need to be adapted to the spatial setting of a one-dimensional lattice where the agent on lattice site k interacts exclusively with the agents located on the neighboring sites $k-1$ and $k+1$. Each sum in (7) over $i \neq k$ then reduces to two terms, so we obtain, for $A_k(t)$ [with similar equations for $B_k(t)$ and $C_k(t)$],

$$\partial_t A_k = (A_{k+1} + A_{k-1})B_k - (C_{k+1} + C_{k-1})A_k. \qquad (14)$$

Introducing the finite difference $\Delta^2 A_k = (A_{k+1} - A_k) - (A_k - A_{k-1})$ allows us to recast this equation in the

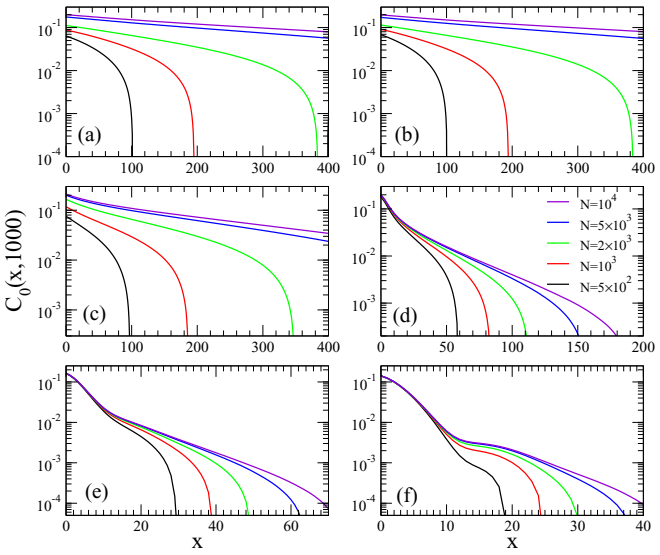

FIG. 4. (Color online) Spatial covariance at time $t = 1000$ for different numbers of balls β [increasing from (a) 1 to (f) 6] and different system sizes. The data result from averaging over 500 000 independent runs.

form

$$\partial_t A_k = (\Delta^2 A_k)B_k - (\Delta^2 C_k)A_k + 2(B_k A_k - C_k A_k). \quad (15)$$

Taking the spatial continuum limit, where we approximate Δ by $a\,\partial_x$, yields the following set of partial differential equations:

$$\begin{aligned}
\partial_t A(x,t) &= \left[\partial_x^2 A(x,t)\right]B(x,t) - \left[\partial_x^2 C(x,t)\right]A(x,t) \\
&\quad + 2[B(x,t)A(x,t) - C(x,t)A(x,t)], \\
\partial_t B(x,t) &= \left[\partial_x^2 B(x,t)\right]C(x,t) - \left[\partial_x^2 A(x,t)\right]B(x,t) \\
&\quad + 2[C(x,t)B(x,t) - A(x,t)B(x,t)], \\
\partial_t C(x,t) &= \left[\partial_x^2 C(x,t)\right]A(x,t) - \left[\partial_x^2 B(x,t)\right]C(x,t) \\
&\quad + 2[A(x,t)C(x,t) - B(x,t)C(x,t)],
\end{aligned} \quad (16)$$

where we set the length scale $a = 1$. This set of equations can straightforwardly be generalized to d dimensions. The terms ∂_x^2 describe the diffusion of strategies through interactions, as the loser of an interaction changes their probability distribution in favor of the strategy against which they lost. The remaining terms are nothing else than the mean-field equations of the normal three-species cyclic game in the well-mixed case.

In Fig. 5(a) we show the numerical solutions of this set of equations for the initial condition

$$\begin{aligned}
A(x,t=0) &= \tfrac{1}{2}\Theta(N/5 - |x - N/2|), \\
B(x,t=0) &= \tfrac{1}{2}\Theta(N/4 - |x - N/2|), \\
C(x,t=0) &= 1 - A(x,t=0) - B(x,t=0),
\end{aligned} \quad (17)$$

where $\Theta(\cdots)$ is the Heaviside step function. In this initial state large segments of the system are occupied by agents that play the same initial strategy. For comparison we show in Fig. 5(b) a numerical simulation for $\beta = 10^6$ balls and the same initial condition. As expected, a system with such a large number of balls is well described by the mean-field equations. The space-time plots in Fig. 5 show that the spatial system with a continuous probability distribution synchronizes very rapidly, yielding spatially extended regions where the probability distribution of every agent is very similar. As a result, the strategies in the whole system coherently oscillate in time. This synchronization effect, which is independent of the initial condition, is readily understood from Eqs. (16) by remarking that the diffusion terms efficiently smooth out the spatial inhomogeneities in the probability distributions until only the well-mixed terms describing the standard rock-paper-scissors interactions matter.

IV. MIXING OF FOUR STRATEGIES

It results from the reactions (1) that in the cyclic Lotka-Volterra scheme with four strategies, pairs of mutually neutral strategies are encountered, as the strategies A and C (B and

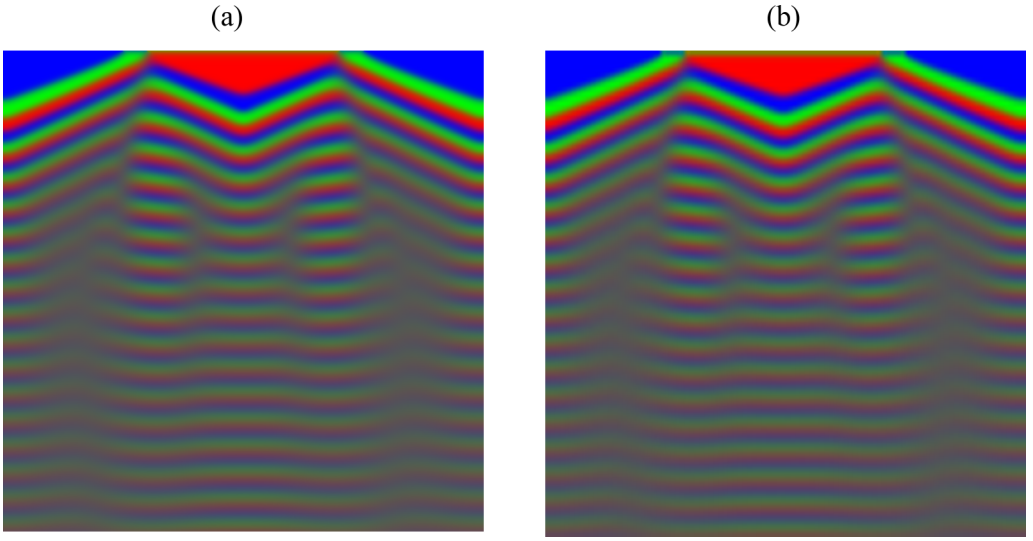

FIG. 5. (Color online) Space-time plots from (a) numerical integration of the spatial mean-field equations (16) and (b) the numerical simulation of a system of 100 lattice sites over 100 time steps with $\beta = 10^6$ balls at each site. In both cases the same initial condition (17) was used. Time increases in the downward direction. The system rapidly synchronizes and coherent waves are formed.

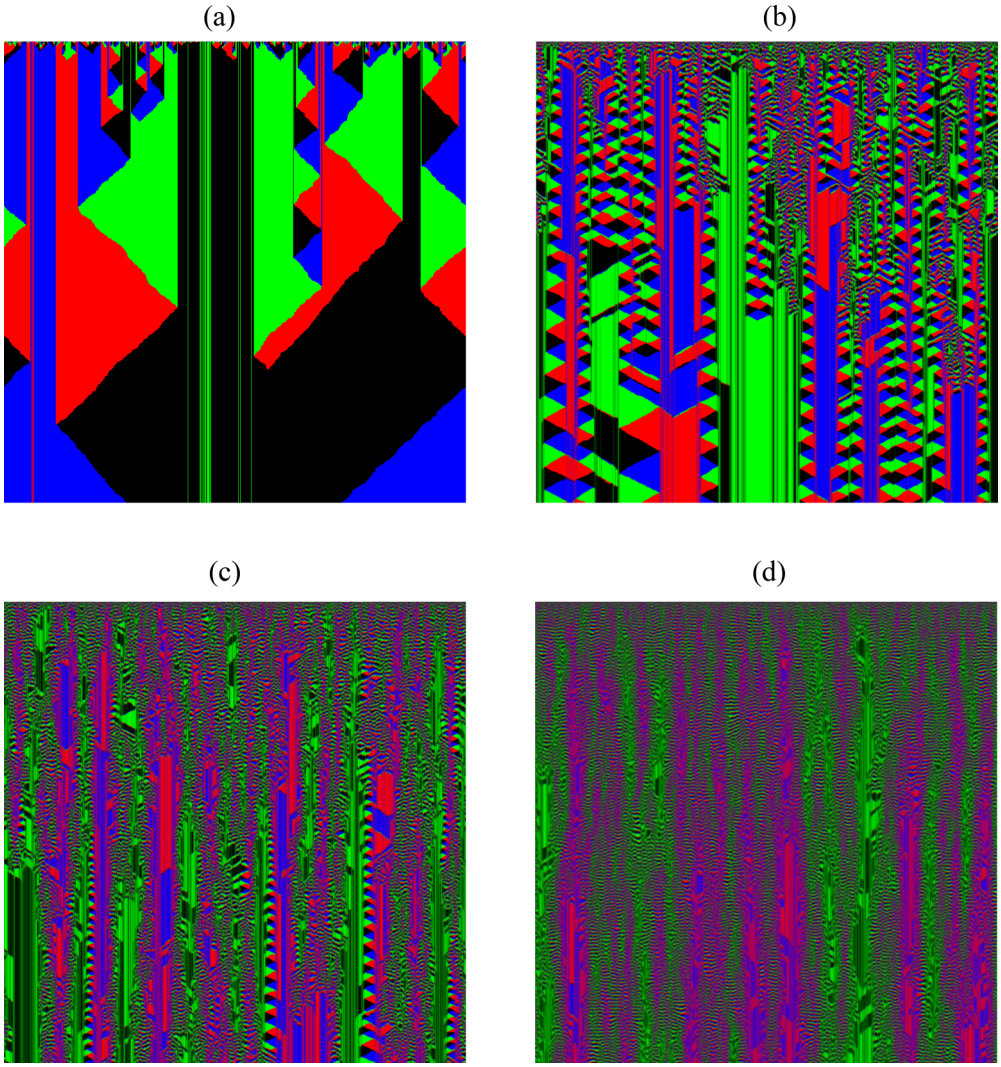

FIG. 6. (Color online) Space-time plots for four-strategy games on a ring with different numbers of balls β on each site: (a) $\beta = 1$, (b) $\beta = 10$, (c) $\beta = 20$, and (d) $\beta = 50$. Time progresses from top to bottom. Shown are 1000 time steps for systems composed of 1000 sites. To determine the color of a lattice site we use the RGB color model and map the percentage of A, B, and C to the percentage of the colors red, green, and blue, respectively. This is adequate as the percentage of D is readily obtained from the fact that the sum over all four densities is 1.

D) do not compete against each other [80]. In the case of pure strategies, this partnership formation yields in a spatial game the formation of domains composed of neutral partners [33] as an agent with a given strategy takes advantage of the fact that its neutral partner plays a strategy that beats the strategy against which the agent would lose. This guiding principle also holds true when considering a four-strategy mixed game with time-dependent probability distributions. Still, remarkable changes in the domain structure and in the mean lattice domination time take place when changing the level of discretization of the probability distribution by increasing β.

A first impression of the changes that happen when the number of balls β is increased can be gained from the space-time plots shown in Fig. 6. For $\beta = 1$ we see the formation of regions dominated by neutral pairs (red and blue vs green and black). As there is no mechanism for mobility, red and blue (green and black) single-species regions become stuck within one another, forming superdomains of neutral partners [78,79]. As a result, a winning strategy can invade the region of a losing strategy only until it hits a patch occupied by the partner strategy of the losing strategy. This results in the zigzaglike structures where the different strategies (in the order red, black, blue, and green) dominate one after the other over a region of the lattice. These regions grow in extent after each change of strategy, yielding ultimately a lattice occupied by only one of the partnerships (either red and blue or green and black). As we increase β, domains of neutral pairs become effectively mixed and a third strategy has a higher probability to invade a superdomain occupied by a given alliance. This results in a much slower growth of the neutral pair domains. Further increasing β causes the neutral species pairs to become very well mixed, resulting in two types of neutral-species domains that overall look purple and dark green. These neutral-species domains continue to compete against each other, yielding a slow coarsening process. Within these coarsening domains cyclic processes continue unabated,

as revealed by the appearance of localized wave patterns for very large β [see Fig. 6(d)]. These waves are very much like those encountered in the three-species case, albeit of smaller extent, only that now one cycles through four types of balls instead of three.

For a more quantitative discussion we turn again to the space-time covariance of the form

$$C_{XY}(x,t) = \frac{1}{N}\sum_i X_i(t)Y_{i+x}(t) - \mu_X(t)\mu_Y(t), \qquad (18)$$

which yields the self-covariance if the species X and Y are the same [see Eq. (13)] and the cross covariance otherwise. We then define an *individual* spatial covariance through the equation

$$C_i(x,t) = \tfrac{1}{4}[C_{AA}(x,t) + C_{BB}(x,t) + C_{CC}(x,t) + C_{DD}(x,t)]. \qquad (19)$$

A different spatial covariance can be obtained when we do not distinguish anymore between neutral strategies but consider them to form a unique group, i.e., strategies A and C together form the group denoted by $\mathcal{A}$, whereas B and D make up the group $\mathcal{B}$. We call the space-time covariance for these larger groups

$$C_n(x,t) = \tfrac{1}{2}[C_{\mathcal{AA}}(x,t) + C_{\mathcal{BB}}(x,t)] \qquad (20)$$

the *neutral* spatial covariance. From these two quantities we can extract two different time-dependent length scales $L_i(t)$ and $L_n(t)$ that provide some insight into the ordering of the superdomains formed by neutral partners. These lengths are obtained from the intersection of the normalized covariance $C_i(x,t)/C_i(0,t)$ and $C_n(x,t)/C_n(0,t)$ with a line of a constant value k, i.e., $C_i(L_i(t),t)/C_i(0,t) = k$ and similarly for $L_n(t)$. We use in the following $k = 0.5$ after carefully checking that the qualitative features discussed below do not depend on the precise value of k.

Figure 7 shows the time evolution of these two lengths for different values of β. Let us first look at the pure case with $\beta = 1$, as we can compare for this case our lengths with those discussed previously in the literature. As shown by Frachebourg *et al.* [79], one needs to consider two different types of domains for the four-species Lotka-Volterra model with immobile particles on a one-dimensional chain: the pure domains occupied by a single species and the superdomains shared by two noninteracting species. Starting from a fully disordered state, the pure domains increase as $t^{1/3}$, whereas the superdomain size, i.e., the distance between active interfaces, is proportional to $t^{2/3}$. As can be seen in Fig. 7(a), for the case $\beta = 1$ both lengths $L_i(t)$ and $L_n(t)$ provide essentially the same information on the superdomains: They are proportional and both display an algebraic increase with an exponent $2/3$ before saturating due to finite-size effects.

Increasing β yields a slowing down of the coarsening process as manifested by a gradual decrease of the exponent governing the growth of the two lengths. For $\beta = 5$, for example, the effective exponent before the transition to the saturation regime is close to 0.45 [see Fig. 7(b)]. This decrease of the exponent describing the long-time regime before saturation continues when further increasing β, with a value of 0.14 for $\beta = 15$ and 0.05 for $\beta = 30$ [see Figs. 7(c) and 7(d)]. This very slow increase for large β is not size dependent and therefore should not be confused with the finite-size plateau seen, for example, in Fig. 7(a) for $\beta = 1$. The very weak increase of the correlation length for large β and large t instead indicates that domain growth almost comes to a standstill due to strong mixing effects. Interestingly, for large β this long-term regime is preceded by another regime where L_n increases as a square root of time [indicated by the red segments in Figs. 7(c) and 7(d)], whereas L_i displays some nontrivial features that reflect the complicated ordering processes seen in the space-time plots. We tentatively identify this regime with the initial formation and growth of the neutral-species superdomains followed by a coarsening process where essentially only two types of domains compete against each other.

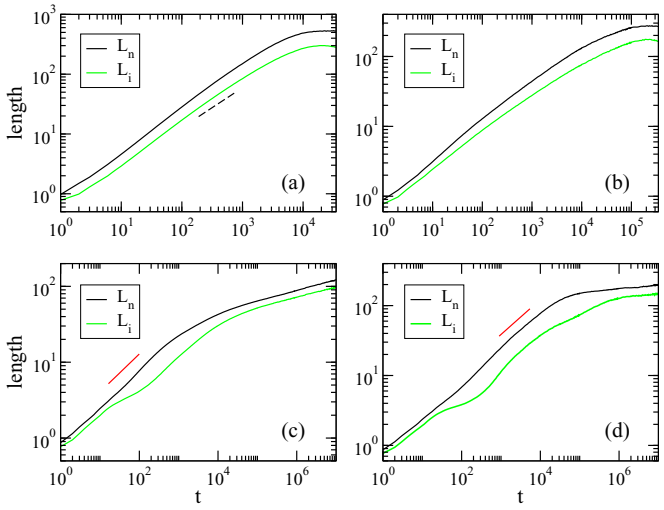

FIG. 7. (Color online) Time-dependent lengths extracted from the space-time covariance for the four-strategy mixed model on a one-dimensional lattice for different values of β: (a) $\beta = 1$, (b) $\beta = 5$, (c) $\beta = 15$, and (d) $\beta = 30$. The length scale L_i (L_n) is obtained from the individual (neutral) spatial covariance. In (a) the system size is $N = 5000$, whereas in (b)–(d) data for a system of 2500 sites are shown. The data result from averaging over typically a few thousand independent runs. In (a) the dashed line indicates an exponent of $2/3$, whereas in (c) and (d) the short red lines indicate an algebraic growth with an exponent of $1/2$.

Another way to characterize these systems is through the study of lattice domination events. The lattice domination time shown in Fig. 8 is the mean number of time steps needed until only one neutral species pair remains in the system. Interestingly, different regimes also show up in the lattice domination time when changing the value of β. For $\beta = 1$, i.e., the case of pure strategies, the lattice domination time increases with the system size as $N^{1.40}$ [37], making this a neutrally stable system. Increasing β slightly changes the exponent (for $\beta = 4$ its value is 1.68), but has no other effect on the lattice domination time. For $\beta \geqslant 5$, however, different regimes emerge as a function of the system size, as shown in Fig. 8(a). Plotting the lattice domination time against the total number of balls in the system $N\beta$ reveals a first regime where the lattice domination time increases algebraically with an exponent close to 2. This is followed by a crossover to a second

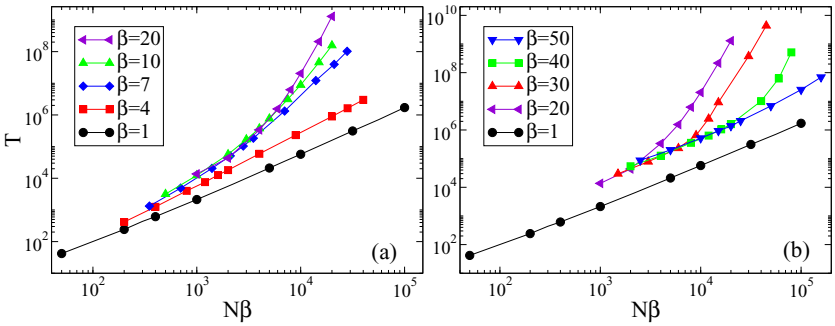

FIG. 8. (Color online) Average lattice domination time as a function of the total number of balls $N\beta$ in the system. Each data point results from an average over 2000 runs, the standard error being smaller than the sizes of the symbols.

algebraic regime with a much larger exponent (for example, for $\beta = 30$ the exponent is 5.60). For β not too large, this crossover takes place at rather similar values of $N\beta$, i.e., the larger β is, the smaller the system size needed to enter the second algebraic regime. Figure 8(b) displays another change of behavior for values of $\beta > 20$, as the crossover is then shifted to larger values of $N\beta$ when increasing β. For the smaller sizes, i.e., before the crossover, the data for different β values fall on one common curve with an exponent of approximately 1.5.

The emergence of two regimes in the lattice domination time for $\beta \geqslant 5$ can be related to different types of extinction events linked to the prevailing domain structure. In small systems extinction can take place at rather short times since the preparation of the system, due to the formation of a few superdomains followed by a coarsening of these domains. For larger N many such domains are formed, resulting in complicated processes dominated by triangular (zigzag) space-time patterns such as those seen in Fig. 6(b) for $\beta = 10$. This periodic cycling through triangles of all four ball types yields a very slow coarsening process. A further increase of β results in the replacement in this second regime of the triangular structures by very long-lived wave patterns, due to some spatially localized synchronization, that dominate the purplish and dark green domains in Fig. 6(d). Domains grow very slowly in that regime [see the late-time behavior of the growth length shown in Fig. 7(d)] and extinction events are only encountered at very late times.

In [37] we showed for the four-species model with pure strategies ($\beta = 1$) that much can be learned about extinction events when studying the probability distribution of the lattice domination time. We expect this to be also true for the more complicated cases with β large. However, the extremely large values of the domination times make it impossible with the resources at our disposal to perform enough runs for a reliable computation of this probability distribution.

V. CONCLUSION

Systems composed of multiple species that interact in a cyclic way have been at the center of a multitude of studies in recent years. Mostly discussed in the context of evolutionary game theory and population dynamics, these systems allow us to understand some of the generic properties arising from nontrivial interactions in ecological systems.

In this paper we discussed a version of the three- and four-species Lotka-Volterra model where the agents are using a mixed strategy, i.e., agents play a pure strategy using a probability distribution every time they interact. Taking into account that agents, both in ecology and economics, tend to learn from past experience, we considered time-dependent probability distributions where a losing agent decreases the probability to play a losing strategy at the next interaction. In order to do so, we treated an agent as an urn containing β balls of three and four types, respectively, where each type corresponds to one of the three or four strategies, respectively. If a strategy loses, a ball of the corresponding type is replaced by a ball with the winning strategy. The number of balls β in the urn therefore measures the level of discretization of the probability distribution, with the limit $\beta \to \infty$ corresponding to a continuous distribution.

As our study revealed, some remarkable changes take place when changing the level of discretization. For the three-strategy case on a one-dimensional lattice we observed a transition between neutrally stable for $\beta \leqslant 3$, where the average time needed for one strategy to completely pervade the system grows algebraically with the system size due to coarsening of single domains, to stable for $\beta > 3$, where this time increases exponentially with the extent of the system, thus indicating the existence of a stable attractor in the coexistence region. This transition gives rise to a change of space-time patterns and the emergence of a tiling structure where strategies dominate for a finite amount of time over certain regions of the lattice. In the limit $\beta \gg 1$, when the probability distribution approximates a continuous distribution, this tiling structure evolves into spatially extended waves where the dominating strategy changes periodically. Synchronization throughout the system is also encountered in the case without spatial dependence and can be understood in the mean-field limit of an infinite number of agents using continuous probability distributions by analyzing the corresponding rate equations. Comparing our three strategy results to those found in [16] for a related multiple-occupancy model, we found a much richer dynamics and a transition in the stability properties of fully occupied lattices when changing the occupancy parameter β.

The four-strategy case is characterized by the existence of pairs of noninteracting strategies. As a result, agents in a spatial setting with $\beta = 1$ want to ally themselves with agents that play the complementary strategy in order to fight off the competing pair of strategies. A direct consequence of this rivalry between competing alliances is the formation and coarsening of superdomains occupied by a single alliance. In contrast to the three-strategy case, an increase of β does not

yield a stable system. Instead, the mean lattice domination time, i.e., the average time needed for one alliance to completely fill the system, always increases algebraically with $N\beta$. Still, different regimes can be identified as a function of N and β. For example, for large values of these parameters a very slow coarsening process is observed, with local synchronized waves within the competing domains.

Besides some results for the well-mixed case without spatial setting, we focused in this paper on the one-dimensional lattice. It is well known from cases with $\beta = 1$ that the dimensionality of the lattice can have a huge impact on the properties of the system. Taking into account the already complex behavior observed in our study of the ring, we expected the appearance of additional intriguing features, especially for the four-strategy case, when considering systems with time-dependent probability distributions in two space dimensions.

In our paper we only considered immobile agents. This is of course not a realistic description for ecological systems. For the Lotka-Volterra-type models considered here, mobility can be implemented through the swapping of agents occupying neighboring lattice sites. It would be interesting to see how the different regimes are modified when allowing for exchanges of agents. We expect to return to that question in the future.

We have restricted ourselves to the simple three- and four-species Lotka-Volterra models with time-dependent probability distribution, as for these situations the properties for the case $\beta = 1$ are well understood and provide a case against which we can study changes that emerge when using a time-dependent probability distribution to play a strategy. Recently there has been a strong focus on more complicated situations, with more species and/or more complex interaction schemes. It is an interesting question how the properties of these systems change when considering a mixed-strategy game with a time-dependent probability distribution. We expect this to be a very fruitful research avenue for the future.

ACKNOWLEDGMENTS

We thank Uwe C. Täuber and Qian He for helpful discussions. This work was supported by the US National Science Foundation through Grant No. DMR-1205309.

APPENDIX: MEAN-FIELD EQUATIONS FOR THE THREE-SPECIES CASE AND $N \to \infty$

For the well-mixed case the first of the three equations in (7) can be rewritten as

$$\begin{aligned}\partial_t A_k(t) &= 2\left(\frac{1}{N-1}\sum_{i\neq k} A_i(t)\right) B_k(t) \\ &\quad - 2\left(\frac{1}{N-1}\sum_{i\neq k} C_i(t)\right) A_k(t) \\ &= \frac{2}{N-1}\left(B_k\sum_i^N A_i - A_k\sum_i^N C_i - B_kA_k + A_kC_k\right) \\ &= \frac{2}{N-1}(B_kN\langle A\rangle_N - A_kN\langle C\rangle_N - B_kA_k + A_kC_k) \\ &= 2\Bigg(B_k\frac{N}{N-1}\langle A\rangle_N - A_k\frac{N}{N-1}\langle C\rangle_N \\ &\quad + \frac{A_kC_k - B_kA_k}{N}\Bigg), \end{aligned} \tag{A1}$$

where $\langle\cdots\rangle_N$ denotes a mean over all agents (urns) in the system. Taking $N \to \infty$ and making the index k continuous yields

$$\partial_t A(x,t) = 2B(x,t)\langle A(x,t)\rangle_x - 2A(x,t)\langle C(x,t)\rangle_x, \tag{A2}$$

where $\langle\cdots\rangle_x = \frac{\int(\cdots)dx}{\int dx}$ indicates an average over the continuous index x. Finally, applying $\langle\cdots\rangle_x$ on both sides of Eq. (A2) yields

$$\begin{aligned}\partial_t\langle A(x,t)\rangle_x &= 2\langle B(x,t)\rangle_x\langle A(x,t)\rangle_x - 2\langle A(x,t)\rangle_x\langle C(x,t)\rangle_x, \\ \partial_t\langle B(x,t)\rangle_x &= 2\langle C(x,t)\rangle_x\langle B(x,t)\rangle_x - 2\langle B(x,t)\rangle_x\langle A(x,t)\rangle_x, \\ \partial_t\langle C(x,t)\rangle_x &= 2\langle A(x,t)\rangle_x\langle C(x,t)\rangle_x - 2\langle C(x,t)\rangle_x\langle B(x,t)\rangle_x, \end{aligned} \tag{A3}$$

where the second and third equations follow from symmetry. These are exactly the mean-field equations for the three-species well-mixed case.

[1] J. Maynard Smith, *Evolution and the Theory of Games* (Cambridge University Press, Cambridge, 1982).
[2] J. Hofbauer and K. Sigmund, *Evolutionary Games and Populations Dynamics* (Cambridge University Press, Cambridge, 1998).
[3] M. A. Nowak, *Evolutionary Dynamics* (Belknap, Cambridge, 2006).
[4] S. Hummert, K. Bohl, D. Basanta, A. Deutsch, S. Werner, G. Theißen, A. Schroeter, and S. Schuster, Mol. Biosyst. **10**, 3044 (2014).
[5] G. Szabó and G. Fáth, Phys. Rep. **446**, 97 (2007).
[6] E. Frey, Physica A **389**, 4265 (2010).
[7] A. Roman, D. Dasgupta, and M. Pleimling, Phys. Rev. E **87**, 032148 (2013).
[8] A. Szolnoki, M. Mobilia, L.-L. Jiang, B. Szczesny, A. M. Rucklidge, and M. Perc, J. R. Soc. Interface **11**, 20140735 (2014).
[9] T. Reichenbach, M. Mobilia, and E. Frey, Nature (London) **448**, 1046 (2007).
[10] T. Reichenbach, M. Mobilia, and E. Frey, Phys. Rev. Lett. **99**, 238105 (2007).
[11] M. Peltomäki and M. Alava, Phys. Rev. E **78**, 031906 (2008).
[12] T. Reichenbach and E. Frey, Phys. Rev. Lett. **101**, 058102 (2008).

[13] S. Venkat and M. Pleimling, Phys. Rev. E **81**, 021917 (2010).
[14] H. Shi, W.-X. Wang, R. Yang, and Y.-C. Lai, Phys. Rev. E **81**, 030901(R) (2010).
[15] W.-X. Wang, Y.-C. Lai, and C. Grebogi, Phys. Rev. E **81**, 046113 (2010).
[16] Q. He, M. Mobilia, and U. C. Täuber, Phys. Rev. E **82**, 051909 (2010).
[17] A. A. Winkler, T. Reichenbach, and E. Frey, Phys. Rev. E **81**, 060901(R) (2010).
[18] Q. He, M. Mobilia, and U. C. Täuber, Eur. Phys. J. B **82**, 97 (2011).
[19] S. Rulands, T. Reichenbach, and E. Frey, J. Stat. Mech. (2011) L01003.
[20] W.-X. Wang, X. Ni, Y.-C. Lai, and C. Grebogi, Phys. Rev. E **83**, 011917 (2011).
[21] J. R. Nahum, B. N. Harding, and B. Kerr, Proc. Natl. Acad. Sci. USA **108**, 10831 (2011).
[22] L. L. Jiang, T. Zhou, M. Perc, and B. H. Wang, Phys. Rev. E **84**, 021912 (2011).
[23] Q. He, U. C. Täuber, and R. K. P. Zia, Eur. Phys. J. B **85**, 141 (2012).
[24] J. Juul, K. Sneppen, and J. Mathiesen, Phys. Rev. E **85**, 061924 (2012).
[25] L.-L. Jiang, W.-X. Wang, Y.-C. Lai, and X. Ni, Phys. Lett. A **376**, 2292 (2012).
[26] D. Lamouroux, S. Eule, T. Geisel, and J. Nagler, Phys. Rev. E **86**, 021911 (2012).
[27] M. W. Adamson and A. Y. Morozov, Bull. Math. Biol. **74**, 2004 (2012).
[28] J. Juul, K. Sneppen, and J. Mathiesen, Phys. Rev. E **87**, 042702 (2013).
[29] S. Rulands, A. Zielinski, and E. Frey, Phys. Rev. E **87**, 052710 (2013).
[30] B. Szczesny, M. Mobilia, and A. M. Rucklidge, Europhys. Lett. **102**, 28012 (2013).
[31] S. J. Schreiber and T. P. Killingback, Theor. Pop. Biol. **86**, 1 (2013).
[32] B. Szczesny, M. Mobilia, and A. M. Rucklidge, Phys. Rev. E **90**, 032704 (2014).
[33] A. Roman, D. Konrad, and M. Pleimling, J. Stat. Mech. (2012) P07014.
[34] G. Szabó and G. A. Sznaider, Phys. Rev. E **69**, 031911 (2004).
[35] G. Szabó, A. Szolnoki, and G. A. Sznaider, Phys. Rev. E **76**, 051921 (2007).
[36] G. Szabó and A. Szolnoki, Phys. Rev. E **77**, 011906 (2008).
[37] B. Intoy and M. Pleimling, J. Stat. Mech. (2013) P08011.
[38] N. C. Guisoni, E. S. Loscar, and M. Girardi, Phys. Rev. E **88**, 022133 (2013).
[39] G. Szabó and T. Czárán, Phys. Rev. E **63**, 061904 (2001).
[40] G. Szabó and T. Czárán, Phys. Rev. E **64**, 042902 (2001).
[41] G. Szabó, J. Phys. A: Math. Gen. **38**, 6689 (2005).
[42] M. Perc, A. Szolnoki, and G. Szabó, Phys. Rev. E **75**, 052102 (2007).
[43] G. Szabó, A. Szolnoki, and I. Borsos, Phys. Rev. E **77**, 041919 (2008).
[44] P. P. Avelino, D. Bazeia, L. Losano, and J. Menezes, Phys. Rev. E **86**, 031119 (2012).
[45] P. P. Avelino, D. Bazeia, L. Losano, J. Menezes, and B. F. Oliveira, Phys. Rev. E **86**, 036112 (2012).
[46] P. P. Avelino, D. Bazeia, J. Menezes, and B. F. de Oliveira, Phys. Lett. A **378**, 393 (2014).
[47] S. Mowlaei, A. Roman, and M. Pleimling, J. Phys. A: Math. Theor. **47**, 165001 (2014).
[48] J. Vukov, A. Szolnoki, and G. Szabó, Phys. Rev. E **88**, 022123 (2013).
[49] Y. B. Kang, Q. H. Pan, X. T. Wang, and H. F. Me, Physica A **392**, 2652 (2013).
[50] P. P. Avelino, D. Bazeia, L. Losano, J. Menezes, and B. F. de Oliveira, Phys. Rev. E **89**, 042710 (2014).
[51] P. Szabó, T. Czárán, and G. Szabó, J. Theor. Biol. **248**, 736 (2007).
[52] A. F. Lütz, S. Risau-Gusman, and J. J. Arenzon, J. Theor. Biol. **317**, 286 (2013).
[53] A. Provata, G. Nicolis, and F. Baras, J. Chem. Phys. **110**, 8361 (1999).
[54] J. Vandermeer and S. Yitbarek, J. Theor. Biol. **300**, 48 (2012).
[55] J. Knebel, T. Krüger, M. F. Weber, and E. Frey, Phys. Rev. Lett. **110**, 168106 (2013).
[56] A. Dobrinevski, M. Alava, T. Reichenbach, and E. Frey, Phys. Rev. E **89**, 012721 (2014).
[57] H. Cheng, N. Yao, Z.-G. Huang, J. Park, Y. Do, and Y.-C. Lai, Sci. Rep. **4**, 7486 (2014).
[58] M. J. Osborne and A. Rubinstein, *A Course in Game Theory* (Massachusetts Institute of Technology Press, Cambridge, 1994).
[59] P. H. Crowley, J. Theor. Biol. **204**, 543 (2000).
[60] S. M. Flaxman, Trends Ecol. Evol. **15**, 482 (2000).
[61] B. Xu, H.-J. Zhou, and Z. Wang, Physica A **392**, 4997 (2013).
[62] Z. Wang, B. Xu, and H.-J. Zhou, Sci. Rep. **4**, 5830 (2014).
[63] F. Salvetti, P. Patelli, and S. Nicolo, Appl. Soft Comput. **7**, 1188 (2007).
[64] T. W. L. Norman, Theor. Decis. **69**, 167 (2010).
[65] E. Bahel, Econ. Lett. **115**, 401 (2012).
[66] C. H. Hommes and M. I. Ochea, Game Evol. Behav. **74**, 434 (2012).
[67] S. Loertscher, Econ. Lett. **118**, 473 (2013).
[68] G. Szabó and C. Hauert, Phys. Rev. Lett. **89**, 118101 (2002).
[69] G. Szabó and C. Hauert, Phys. Rev. E **66**, 062903 (2002).
[70] Z. Xu, Z. Wang, and L. Zhang, Phys. Rev. E **80**, 061104 (2009).
[71] A. Szolnoki, G. Szabó, and M. Perc, Phys. Rev. E **83**, 036101 (2011).
[72] A. Arenas, J. Camacho, J. A. Cuesta, and R. J. Requejo, J. Theor. Biol. **279**, 113 (2011).
[73] L.-X. Zhong, W.-J. Xu, Y.-D. Shi, and T. Qiu, Chaos Soliton. Fract. **47**, 18 (2013).
[74] T. Killingback and M. Doebeli, Proc. R. Soc. London Ser. B **263**, 1135 (1996).
[75] M. H. Vainstein and J. J. Arenzon, Phys. Rev. E **64**, 051905 (2001).
[76] C. Hauert and M. Doebeli, Nature (London) **428**, 643 (2004).
[77] E. A. Sicardi, H. Fort, M. H. Vainstein, and J. J. Arenzon, J. Theor. Biol. **256**, 240 (2009).

[78] L. Frachebourg, P. L. Krapivsky, and E. Ben-Naim, Phys. Rev. Lett. **77**, 2125 (1996).
[79] L. Frachebourg, P. L. Krapivsky, and E. Ben-Naim, Phys. Rev. E **54**, 6186 (1996).
[80] S. O. Case, C. H. Durney, M. Pleimling, and R. K. P. Zia, Europhys. Lett. **92**, 58003 (2010).
[81] R. M. May and W. J. Leonard, SIAM J. Appl. Math. **29**, 243 (1975).
[82] B. M. F. Intoy, Pure and mixed strategies in cyclic competition: Extinction, coexistence, and patterns, Ph. D. thesis, Virginia Tech, 2015.
[83] A. Dobrinevski and E. Frey, Phys. Rev. E **85**, 051903 (2012).
[84] T. Antal and I. Scheuring, Bull. Math. Biol. **68**, 1923 (2006).
[85] J. Cremer, T. Reichenbach, and E. Frey, New J. Phys. **11**, 093029 (2009).